This article has been accepted for publication in a future issue of this journal, but has not been fully edited. Content may change prior to final publication. Citation information: DOI 10.1109/TAP.2017.2684199, IEEE Transactions on Antennas and Propagation

Frequency Selective Surface Structure Miniaturization Using Interconnected Array Elements on Orthogonal Layers

M. Hussein, *Student member, IEEE,* J. Zhou, Y. Huang, *Member, IEEE*, M. Kod and A. P. Sohrab, *Student member, IEEE*

***Abstract*—Traditionally, the element of a frequency selective surface (FSS) is rotationally symmetrical and the element arrays in a multi-layer FSS are aligned with each other. A new approach to miniaturize the size of the FSS array element is proposed in this paper by interconnecting array elements only in one direction in a two-layer FSS structure. One layer acts as an enhanced inductor while the other layer provides capacitance. The interconnection between adjacent array elements changes the equivalent circuit and produces a strong cross-layer capacitance, which lowers the resonant frequency significantly. The dimensions of the miniaturized FSS element are much smaller than the wavelength at the resonant frequency (periodicity << λ). The element can also have a low profile since the cross-layer capacitance is stronger with a thinner substrate.**

The sensitivity to the incident angle of the proposed structure is comparable with traditional ones. A theoretical equivalent circuit model is developed to characterize the structure, based on analysis of the geometrical configuration of the FSS structure and the electric field distribution on it. The theory was verified by experimental results.

***Index Terms*: Equivalent circuit, frequency selective surfaces, filter, orthogonal, cross-layer capacitor.**

I. INTRODUCTION

FREQUENCY selective surface (FSS) are structures composed of arbitrary shapes of metallic patches or apertures supported by dielectric substrates. FSSs have been the subject of intense investigations in a large scale of applications, such as spatial microwave and optical filters for decades [1-4]. FSS structures often are used as radomes for reducing the radar cross section of an antenna system outside its frequency band of operation. They can also be used as components in radar-absorbing material (RAM) [5-7]. The use of FSSs has contributed to the increase in the communication capabilities of satellite platforms. The use of dual-reflector antennas, which share the main reflector among different frequency bands, in space missions such as Galileo, Cassini and Voyager, has been made possible by using an FSS [8-10]. Decreasing power loss in antennas and improving the radiated power are successfully realized by using these structures[11].

Manuscript received Jun. 21, 2016; revised Sep. 24, 2016. The authors are with the Department of Electrical Engineering and Electronics, The University of Liverpool, UK. (e-mail:Jiafeng.Zhou@liverpool.ac.uk).

The geometry of the surface in one period (array element) determines the frequency response of an FSS. Various responses can be achieved by using different FSS element shapes. The equivalent circuit and analysis of some of the traditional structures are provided in [12, 13]. The equivalent FSS circuit is directly related to the array element shape and the polarization. An FSS is essentially a spatial filter because its performance depends on frequency, polarization and the angle of incidence. FSSs often display selectivity not only to frequency, but also to the angle and polarization of the incident wave.

However, the FSS suffers from practical design problems that can be categorized as the bandwidth, the size of the element, the sensitivity to the incident angle and the sensitivity to the polarization. The reflection and transmission coefficients of the FSS are mainly dependent on the shape and size of array elements. The electrical length of the array elements is an essential factor to determine the resonant frequency. It is important that the shape, dimensions and spacing of the array elements are designed altogether to achieve the desired resonant frequency and bandwidth.

Recently, many approaches have been proposed to miniaturize FSS array element dimensions. For example, a lumped inductor and a lumped capacitor in parallel can be used to reduce the size of FSS array elements [14, 15]. Adding meander-slots to the circular ring structures can produce FSS array element with dimensions much smaller than the wavelength [16]. A study in [17] demonstrated a miniature FSS by printing micro wire on a dielectric. Printing four symmetrical spiral patterns of metallic meander lines can increase the electrical length of the array element [18]. However, increasing the electrical length of an array element with the same physical dimensions is limited, and could increase the complexity of the FSS structure.

Different techniques have been used to achieve stable frequency responses in different polarizations for single and multi-layer FSSs under various angles of incident waves. Accomplishing a symmetrical FSS array element can contribute to achieving a stable resonance with respect to the polarization and the angle of incidence [14-19]. However, using symmetrical array element shapes to avoid polarization sensitivity can restrict FSS design options.

This article has been accepted for publication in a future issue of this journal, but has not been fully edited. Content may change prior to final publication. Citation information: DOI 10.1109/TAP.2017.2684199, IEEE Transactions on Antennas and Propagation

It is proposed in this paper that the size of the FSS element can be miniaturized by connecting adjacent elements in *one* direction only to increase the resonant component values in a two- or multi-layer structure. The proposed miniaturized FSS is able to exhibit the same frequency response with respect of horizontal or vertical polarizations. This is achieved by printing the same metal shape on the top and bottom of the substrate, but orthogonally in a two-layer structure. At the same time, a cross-layer capacitance (C_{cc}) will be generated. This capacitor can significantly lower the resonant component of the FSS. Traditionally, in single or multi-layer structures, the lower the profile, the higher the resonant frequency. This is mainly due to that the effective dielectric constant is gradually increased when the substrate thickness is increased. In contrast, in the proposed structure, the lower the profile, the lower the resonant frequency, due to the increased cross-layer capacitance. The frequency response of the miniaturized FSS is demonstrated for various incident angles. It is shown that the performance is very stable. An analytical model is derived to evaluate the resonant frequency of the proposed miniaturized FSS.

In this paper, section II focuses on the design of array elements, and discusses the proposed approaches to miniaturize the FSS array element. Section III describes the experiment setup and measured results to verify the theory. Conclusions are finally given in Section IV.

II. Miniaturization Approaches

A. Array Element Design

The miniaturization of FSS elements is desired to enable an FSS with sufficient array elements to act as an infinite array because a practical FSS is usually fabricated in finite dimensions. Many approaches have been used to miniaturize the FSS element. These approaches mainly depend on increasing the electrical length of array elements with the same physical area. However, this could result in a more complex FSS structure.

In this paper, new approaches will be introduced to miniaturize an FSS element. Firstly, the inductance can be enhanced by connecting adjacent elements in one direction. Secondly, an extra capacitor is introduced by having two metallic layers orthogonal to each other. This capacitance enables the FSS to have a much lower profile. The proposed array element is designed in such a way that the connection between adjacent elements is easily achievable. At the same time, the array element in an FSS is not necessarily symmetrical at 90° rotation.

The proposed resonator is a ring with two splits. Each split is ended by two parallel strips. Inside the ring, there is a pair of T-shaped strips with a gap in the center, as shown in Fig.1. However, the structure still works if a simple wire is used in the middle of the unit cell. It was found by parametric study that the whole structure is slightly smaller by using two T-shaped wires instead of a single wire and it provides flexibility to control the stopband frequency. The resonant frequency of the proposed resonator can be easily lowered by interconnecting the elements, to be discussed in detail in the following sections.

B. Enhanced Inductance Array Elements

Fig 1 shows the proposed structure. At the vertical polarization, the electric field is in the direction of the y-axis. The gaps between the two T-shaped strips can be represented by a capacitor, shown as (a) in Fig. 1. Half of the circumference with the parallel strips acts as an inductor, shown as (b). The gap between adjacent elements can be represented by a capacitor, shown as (c). The corresponding equivalent circuit of the resonator, when the incident wave is vertically polarized, consists of a C in parallel with a series LC as shown in Fig 3. C_2 represents the capacitance shown as (a) in Fig. 1. L_1 represents the inductance shown as (b). C_1 represents the capacitance shown as (c).

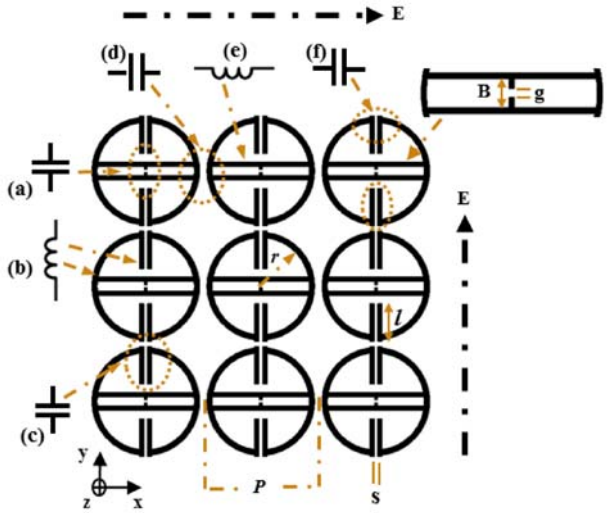

Fig. 1. The proposed structure with not-connected elements.

Similarly, for the horizontal polarization, the equivalent circuit of the resonator can also be described by Fig. 1. In this case, C_1 represents the mutual capacitance between the adjacent elements, shown as (d) in Fig. 1. L_1 is the inductance of the two T-shaped strips shown as (e). C_2 is the capacitance of the parallel strips, shown as (f). The corresponding equivalent circuit of the resonator, when the incident wave is horizontally polarized, is also a C in parallel with a series LC. The equivalent circuit can also be represented by Fig. 2, although the values of the components are different.

To verify the proposed structure, numerical analysis of the proposed element was performed by CST Microwave Studio, using unit cell boundary conditions to provide periodicity along the x and y axes. The FSS is excited by an electromagnetic wave with the propagation vector (**K**) towards the z-axis direction, magnetic field vector (**H**) towards the x–axis direction and electric field vector (**E**) towards the y-axis direction, as shown in Fig. 3. The frequency response of the array elements can be determined by evaluating the capacitance and inductance of the element. The approximate value of the inductance of a strip can be calculated by [20],

$$L = \mu \frac{P}{2\pi} \log\left(\frac{1}{\sin\frac{\pi w}{2P}}\right) \quad (1)$$

This article has been accepted for publication in a future issue of this journal, but has not been fully edited. Content may change prior to final publication. Citation information: DOI 10.1109/TAP.2017.2684199, IEEE Transactions on Antennas and Propagation

where L is the strip inductance, which is determined by the strip length P, the strip width w , and the effective magnetic permeability μ of the structure. The approximate value of the capacitance between strips can be calculated by [20],

$$C = \varepsilon_o \varepsilon_e \frac{2P}{\pi} \log\left(\frac{1}{\sin\frac{\pi g}{2P}}\right) \quad (2)$$

where C is the capacitance between adjacent strips, which is determined by the strip length P, the gap width g between the strips and the effective dielectric constant ε_e of the structure. The effective dielectric constant increases when the substrate thickness is increased. The capacitance between adjacent strips increases if the thickness of the substrate becomes thicker [4], although the increment will be smaller if the thickness of the substrate is much greater than the gap width. On the other hand, the inductance is determined by the length and width of the metallic strip.

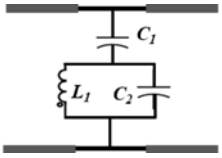

Fig. 2. The equivalent circuit of the proposed FSS unit.

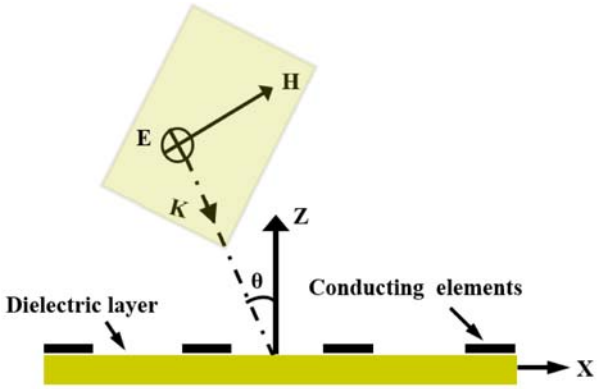

Fig. 3. Side view of the proposed array elements under EM wave illumination. ɵ is the incident angle.

An FSS was designed on a 0.127 mm thick FR4 substrate with a dielectric constant of 4.3. The strip width w is 0.3 mm, s = 0.4 mm, g = 0.25 mm, l = 3.7 mm and B = 0.6 mm, as shown in Fig. 1. The inner and outer ring radius is 4.4 mm and 4.7 mm, respectively. The periodic element P is 10 mm. The simulated performance of the structure of Fig. 1 is shown in Fig. 4. At the vertical polarization, the structure exhibits bandstop performance, and has a resonant frequency of 6.25 GHz, as shown in Fig. 4(a). The resonant components of the equivalent circuit, as shown in Fig. 2, can be calculated by using (1) and (2), where C_1 = 0.772 pF, C_2 = 0.209 pF and L_1 = 0.657 nH. To achieve good agreement with the simulated one, as shown in Fig. 4 (a), a curve fitting was carried out. It was found that by taking C_1 = 0.821 pF and L_1 = 0.663 nH, the calculated response will be in excellent agreement with the simulated one as shown in Fig. 4. These component values are very close to those obtained by calculation using (1) and (2).

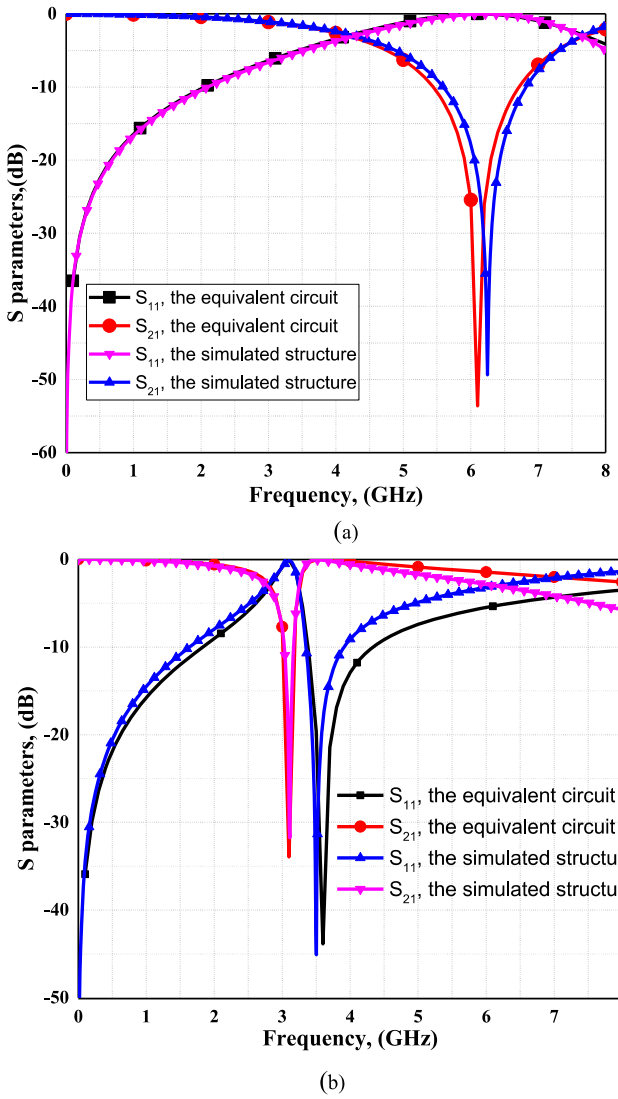

Fig. 4. The transmission and reflection coefficients of the structure shown in Fig. 1, by using the equivalent circuit and simulation, (a) at the vertical polarization, (b) at the horizontal polarization.

At the horizontal polarization, the structure exhibits performance with a stopband at 3.10 GHz and a passband at 3.49 GHz, as can be observed from Fig. 4 (b). The component values in the equivalent circuit are C_1 = 1.02 pF, C_2 = 2.59 pF and L_1 = 0.642 nH as calculated using (1) and (2). By curve-fitting, C_2 is tuned to 2.7 pf to achieve good agreement with the simulated structure, as shown in Fig. 4 (b).

To miniaturize the resonator, the adjacent elements of the proposed structure can be connected in one direction through two parallel strip wires, as shown in Fig. 5. This can enhance the inductance of the proposed structure compared to the case where the elements are not interconnected as shown in Fig. 1. However, the equivalent circuit of the strips in the interconnected array elements is an inductor, as shown in Fig. 5. While as shown in Fig. 1, the strips in the not-interconnected array element have series capacitance associated with the gap between adjacent elements, resulting in the equivalent circuit of

This article has been accepted for publication in a future issue of this journal, but has not been fully edited. Content may change prior to final publication. Citation information: DOI 10.1109/TAP.2017.2684199, IEEE Transactions on Antennas and Propagation

a series *LC* circuit. The simulation for the enhanced-inductance (interconnected) elements, with the circuit dimensions provided above, was carried out. The E-field is assumed to be vertical as shown in Fig. 5. The FSS has a highpass response, as shown in Fig. 6(a), because the equivalent circuit is mainly an inductor as described above.

For the horizontal polarization, the parallel strips in the interconnected circuit can be represented by a capacitor, as shown in Fig. 5. The simulated response of the structure has a bandstop response with a resonant frequency of 2.9 GHz, as shown in Fig. 6(b). The equivalent circuit is a C in series with a parallel LC, as shown in Fig. 2. C_1 represents the mutual capacitance between the adjacent elements, L_1 is the inductance of the two T-shaped strips, and C_2 is the capacitance of the parallel strips, as shown in Fig. 5. The equivalent circuit component values are C_1 = 1.09 pF, L_1 = 0.642 nH. To achieve good agreement with the simulated performance, C_2 is tuned from 2.8 pF to 2.9 pF by curve-fitting.

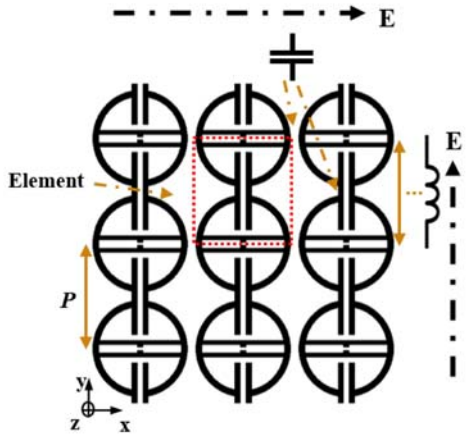

Fig. 5. The proposed structure with the elements interconnected in one direction.

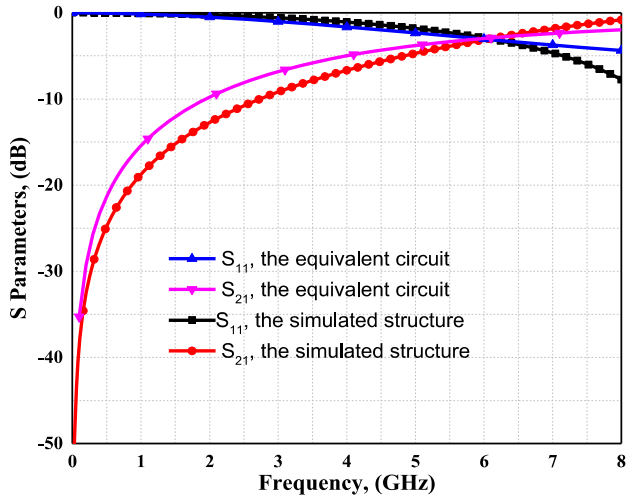

(a)

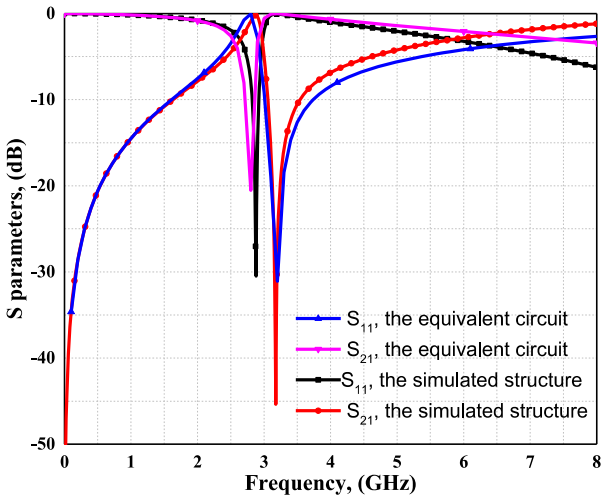

(b)

Fig. 6. The transmission and reflection coefficients of the structure shown in Fig. 5, obtained by calculating the equivalent circuit and simulating the structure, (a) for the vertical polarization, (b) for the horizontal polarization.

In fact, the interconnection between the proposed FSS array elements will not only increase the inductance, but also change the equivalent circuit. That is, the interconnection contributes to making the top layer act as only an inductor (the inductance is dominant) and the bottom layer acts as a capacitor, as discussed in detail in the next section.

C. FSS with Orthogonal Layers in the xy-Plane

Recently, many approaches have been proposed [14-19] to miniaturize array elements by increasing the capacitance or inductance or both. These approaches include increasing the substrate thickness or the complexity of the structures. *The proposed* miniaturized *FSS* in this paper utilizes a metal-dielectric-metal structure to design a passband filter by having two layers of the same shape but arranged orthogonally. In the proposed structure, the top layer of the substrate, as shown in Fig. 5, acts as an inductor for vertical polarization. While, the capacitance is achieved by the bottom layer which is the same as the top layer but with 90° rotation.

More importantly, the structure will exhibit the same transmission performance in the x and y directions. *In this* way, the proposed array element is insensitive to the polarization angle. That is, in the vertical polarization, the metal layer at the top acts as an inductor because the inductance is dominant. At the same time, the bottom metal layer presents a capacitance because the capacitance is dominant. In the horizontal polarization, the top metals layer acts as a capacitor and the bottom metal layer acts as an inductor. The most important advantage is that, by having two layers orthogonally, it can induce a strong capacitance between them. This capacitor is induced because the charge distribution is different between the top and the bottom layers of the FSS. For instance, when an external electrical field, *E*, is applied in the y-axis (vertical) direction, the dominant current will be on the ring circumference toward the y (or -y) axis direction, as shown in Fig. 7(a). The current is the strongest at the edge of the resonator. This can induce positive charges on the top half of the proposed element and negative charges on the bottom half

This article has been accepted for publication in a future issue of this journal, but has not been fully edited. Content may change prior to final publication. Citation information: DOI 10.1109/TAP.2017.2684199, IEEE Transactions on Antennas and Propagation

as shown in Fig. 7(b). On the other hand, for the 90° rotated element on the other layer, the direction of the current is similar to the top layer, but the strongest current is in the center of the resonator, as shown in Fig. 8(a). As a result, the top half of the array element will have negative charges, while the bottom will have positive charges as shown in Fig. 8(b).

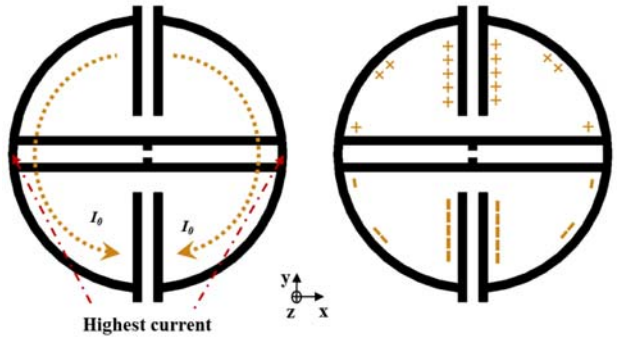

(a) (b)

Fig. 7. (a) The current distribution and (b) the charge distribution on the top layer of the proposed structure for vertical polarization.

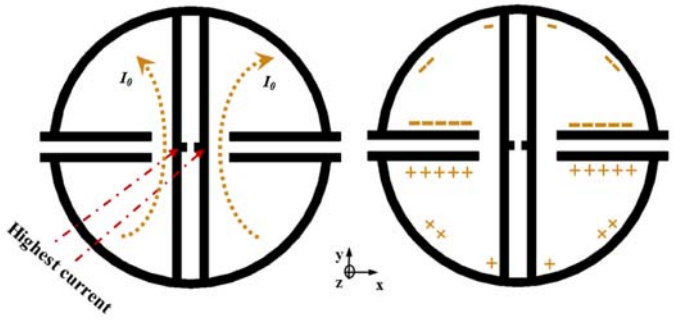

(a) (b)

Fig. 8. (a) The current distribution and (b) the charge distribution on the orthogonal layer of the proposed structure for vertical polarization.

This induces a strong cross-layer capacitance, C_{cc}, between the parallel layers of the proposed array element, as shown in Fig. 9. The equivalent circuit of the unit of the two orthogonal elements is a combination of the equivalent circuit of the top layer (enhanced inductor) and the bottom layer (*C in series with a parallel LC)*, as illustrated in Fig. 10, where L_T is the inductance of the two T-shaped strips, C_e is the capacitance of the parallel strips, and L_e is the enhanced inductor. C_s is the sum of the mutual capacitance, C_m, between the adjacent elements, and the cross-layer capacitance between the top and bottom layers, C_{cc}. Where the cross-layer capacitance can be estimated by:

$$C_{cc} = \frac{\varepsilon_r \varepsilon_o A}{d} \tag{3}$$

where A is the area of the proposed surface. The parallel surfaces are separated by a distance d which is the thickness of the substrate; the dielectric constant of the substrate is ε_r.

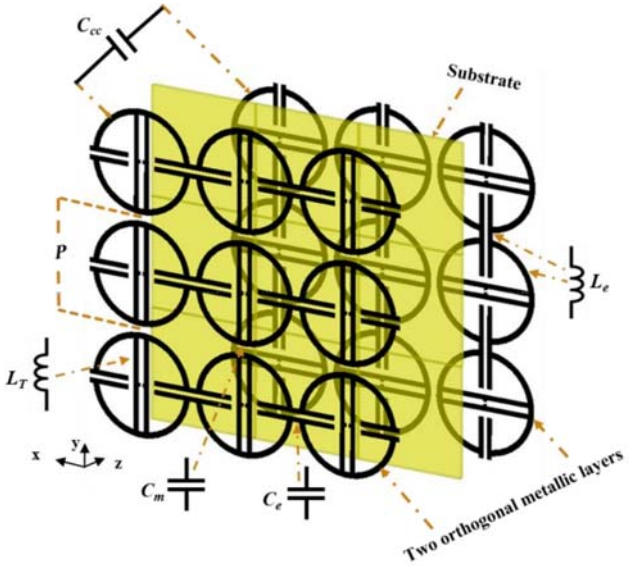

Fig. 9. The array elements are placed orthogonally to each other on adjacent layers. A strong cross-layer capacitance exists between the two layers.

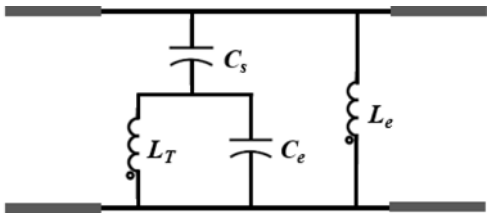

Fig. 10. The equivalent circuit of the proposed miniaturized FSS unit, C_s= the mutual capacitance between adjacent elements (C_m) + the cross-layer capacitance (C_{cc}).

D. Circuit Design

The simulated magnitudes of S_{11} and S_{21} of the proposed structure at 0.127 mm substrate thickness are shown in Fig. 11. The responses in the vertical and horizontal polarizations for the TE mode are almost the same as each other. It is shown in Fig. 12 that the phases of S_{21} are the same as each other as well. Table I shows the simulated resonant frequency, the fractional bandwidth and the array element size as a function of the thickness of the substrate.

It is obvious that decreasing the substrate thickness from 0.8 mm to 0.127 mm can shift the resonant frequency downward from 2.32 GHz to 1.35 GHz. The array element size is miniaturized by 58% (from 0.0773λ to 0.045λ*)*, although there is a small bandwidth decrease.

Table I. Resonant frequencies and element sizes with different substrate thicknesses

Thickness (Unit: mm)	f_r (Unit: GHz)	Fractional bandwidth	Element size
0.8	2.32	11%	0.077λ
0.6	2.18	9.3%	0.073λ
0.3	1.82	8.7%	0.060 λ
0.127	1.35	7.5%	0.045λ

This article has been accepted for publication in a future issue of this journal, but has not been fully edited. Content may change prior to final publication. Citation information: DOI 10.1109/TAP.2017.2684199, IEEE Transactions on Antennas and Propagation

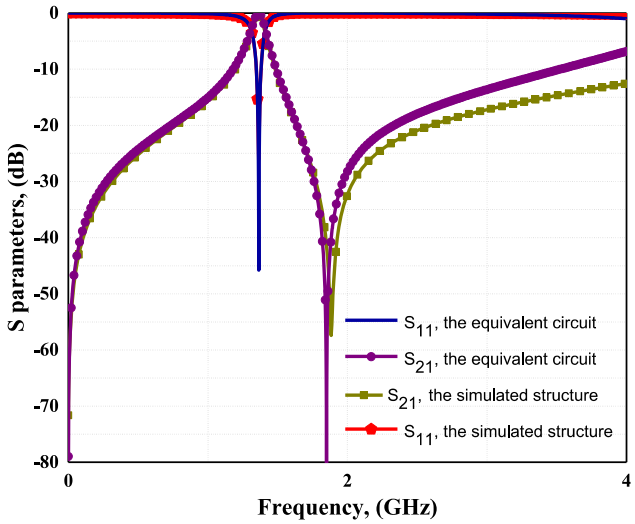

Fig. 11. The simulated and calculated responses of the miniaturized FSS structure. Due to the orthogonal nature of the structure, the performance is the same for both the vertical and the horizontal polarizations.

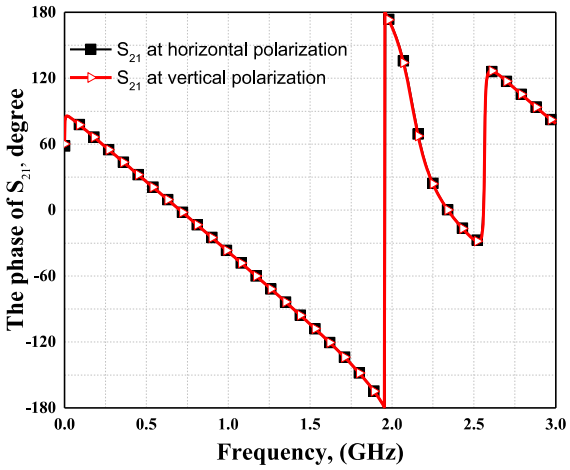

Fig. 12. The simulated phases of the transmission coefficients of the miniaturized FSS structure for both the vertical and the horizontal polarizations.

It should be noted that the low profile can be achieved only if C_{cc} is dominant compared to the adjacent strips' capacitance C_m and C_e. The values of the equivalent circuit components for a 0.127 mm thick substrate are C_m = 1.09 pF, C_e = 2.9 pF, and L_T = 0.642 nH, while from (3) C_{cc} is 6.25 pF as calculated from (3). The value of C_{cc} is much bigger than the adjacent strips' capacitances.

To obtain good agreement with the simulated structure, as shown in Fig. 11, a curve fitting was carried out. While other component values are very close to the calculated ones, the value of C_{cc} is found to be 7.33 pF after curve fitting. This deviation is mainly due to the fringing effect of the field between the edges of two parallel plates. This deviation increases with the thickness of the substrate, especially when $w<<d$. There are several approaches to quantify the fringing effect [21, 22]. The total capacitance including the fringing effect of a circular parallel-plate capacitor can be estimated by [23]:

$$C_{cc} = \varepsilon_r \varepsilon_o [\frac{\pi r^2}{d} + r \ln(\frac{16\pi r}{d} - 1)] \quad (4)$$

where, r is the radius of the circular disk. As a comparison, the calculated capacitance of a circular disk with r= 4.7 mm and

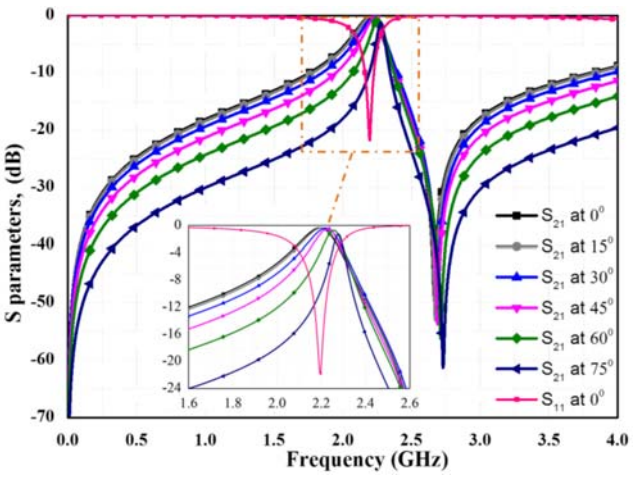

(a)

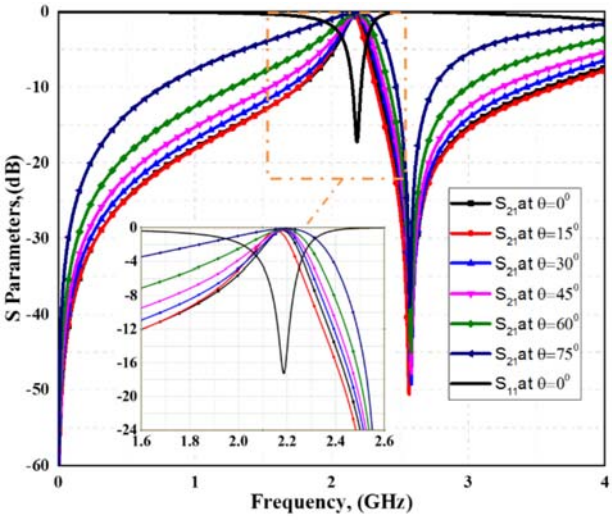

(b)

Fig. 13. The simulated reflection and transmission coefficients of the miniaturized FSS structure as a function of the incident angle, (a) TE mode, (b) TM mode.

d= 0.127 mm would have been 7% higher by considering the fringing effect. For the proposed structure, the value of the capacitance is 17% higher after curve fitting. The deviation in the ring structure is slightly higher because the fringing effect takes place on both the inner and the outer edges of the ring structure. The deviation would also be greater if the substrate is thicker.

The cross-layer capacitance contrasts with the adjacent capacitors (C_m and C_e). C_{cc} would increase if the thickness of the substrate was reduced, while C_m and C_e would decrease.

The structure was simulated under various incident angles and for different modes. The substrate thickness used in the simulation is 0.6 mm. The results show that the resonant frequency is very stable as shown in Fig. 13. The insertion loss

This article has been accepted for publication in a future issue of this journal, but has not been fully edited. Content may change prior to final publication. Citation information: DOI 10.1109/TAP.2017.2684199, IEEE Transactions on Antennas and Propagation

is 0.33 dB at the normal incident angle and 0.69 dB at the 60˚ incident angle for the TE mode. While the insertion loss is 0.32 dB at the normal incident angle and 0.18 dB at 60˚ incident angle for the TM mode. As a comparison, the simulated insertion loss at normal incident angle is 0.35 dB for the TE mode and 0.4 dB for the TM mode; while at 60˚ incident angle, it is 0.5 dB for the TE mode and 0.3 dB for the TM mode, in [15]. The values at the normal incident angle are 0.2 dB for the TE mode and 0 dB for the TM mode; 0.3 dB for the TE mode and 0 dB for the TM mode at 60˚ incident angle in [16], or 1.4 dB for the TE mode and 1.2 dB for the TM mode at the normal incident angle and 1.6 dB for the TE mode and 0.8 dB for the TM mode at 60˚ in [18].The insertion loss of the proposed structure is comparable to the results in other references.

Table II. The deviation of the resonant frequency for different incident angles for the TE mode

Incident angle (Unit: degree)	f_r (Unit: GHz)	Deviation
15º	2.19	0.4%
30º	2.20	0.9%
45º	2.22	1.8%
60º	2.25	3.2%
75º	2.26	3.6%

Table III. The deviation of the resonant frequency for different incident angles for the TM mode

Incident angle (Unit: degree)	f_r (Unit: GHz)	Deviation
15º	2.156	1.10%
30º	2.184	0.183%
45º	2.188	0.367%
60º	2.188	0.367%
75º	2.192	0.550%

Compared with the normal incidence case, the deviations of the resonant frequency of the miniaturized FSS structure at different incident angles, for both TE and TM modes, are shown in the Table II and III, respectively. The resonant frequency is shifted from 2.18 GHz to 2.25 GHz (3.2%) at the 60º incident angle for the TE mode and 0.37% for the TM mode. As a comparison, the resonant frequency deviation is 6.6% for the TE mode at 60˚ incident angle in [14], 2% for both the TE and the TM modes in [15], 0% for the TE mode and 1.3% for the TM mode in [16], and 0% fort the TE mode and 5% for the TM mode in [18].

The simulated result of the transmission coefficients of the miniaturized FSS structure under 45˚ incident angle and various polarization angles is shown in Fig. 14. It can be seen that the transmission coefficient is hardly changed with the polarization angle, although the array element is not rotationally symmetrical by 90˚ as for most traditional elements. This advantage offers great flexibility for the array element design. This methodology can be applied to the design of multi-layer FSSs. For example, a three-layer FSS can be designed by having each layer at an angle of 120˚ to the next layer.

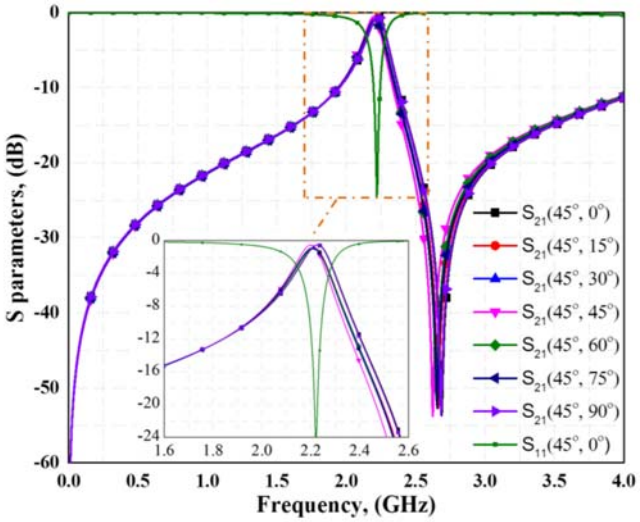

Fig. 14. The simulated reflection and transmission coefficients of the miniaturized FSS structure under incident angle of 45º and various polarization angles.

Cross-polarization levels between TE and TM waves are also examined with regard to normal incident angle and varied polarization angles (0º to 45º). The direction of polarization is rotated from 0◦ to 45◦ to examine the cross-polarization levels at different incident angles. The proposed orthogonal layers present a very low polarization conversion which is generally below -25 dB. The transmission coefficients in cross polarization at the resonant frequency is better than -45 dB at the 0º polarization angle, -40 dB at 15º, -30 dB 30º and -27 at 45º. This confirms that when TE wave propagates through the proposed orthogonal layers, the transmitted wave is still with TE polarization. The performance is similar for the TM case.

A comparison of the FSS array element size between the proposed design and other miniaturized FSS elements described in previous works is illustrated in Table IV. It can be seen that the proposed structure has the smallest size.

Moreover, the effect of the misalignment between the orthogonal layers is simulated. The simulation was carried out by shifting one layer with different distances, as show in Table V. The proposed structure exhibits a stable frequency response to the misalignment. As an example, the resonant frequency was shifted from 2.018 GHz to 2.0204 GHz at 0.5 mm misalignment between the surface layers, as shown in the table.

Table IV. Comparison of element size with other references

FSS structure	Substrate thickness (Unit: mm)	ε_r	Element size
[14]	1.6	4.3	0.22λ
[15]	1.6	4.3	0.104λ
[16]	0.5	3.55	0.088λ
[17]	0.127	2.2	0.067λ
[18]	1.6	5	0.061λ
[19]	1	3	0.058λ
[24]	0.021	1.12	0.266λ
The proposed array element	0.127	4.3	0.043λ

This article has been accepted for publication in a future issue of this journal, but has not been fully edited. Content may change prior to final publication. Citation information: DOI 10.1109/TAP.2017.2684199, IEEE Transactions on Antennas and Propagation

Table V. The deviation of the resonant frequency caused by the misalignment between the top and bottom layers

Misalignment (Unit: wavelength λ)	Misalignment (Unit: mm)	Deviation
0.00145	0.2	0.11%
0.00218	0.3	0.48%
0.0036	0.5	1.1%

The bandwidth of the proposed design is relatively narrow. In some applications, a wider wideband performance might be desired. The proposed techniques can be adopted to design a wideband FSS as well. This can be done by changing the dimensions of the circuit to tune the *LC* values. As the equivalent circuit is L-C in parallel, decreasing the total capacitance value will increase the bandwidth, while decreasing the inductance will decrease the bandwidth. For the proposed structure, one easy way to achieve a wider passband is to decrease the strip width to tune the *LC* values. For example, for the proposed structure with 0.6 mm thickness, the bandwidth is doubled by decreasing the strip width (w) from 0.3 mm to 0.02mm, as shown in Table VI. If it is difficult to fabricate such narrow strips, the FSS element can be revised to achieve a wider bandwidth, which can be the topic of a future publication.

Table VI. Fractional bandwidths and element sizes with different strip widths at 0.6 mm substrate thickness

W (Unit: mm)	f_r (Unit: GHz)	Fractional bandwidth	Element size
0.3	2.18	9.3%	0.077λ
0.1	2.39	14%	0.079λ
0.05	2.44	17.5%	0.081λ
0.02	2.47	19%	0.082 λ

III. Experimental Results

The proposed FSS was fabricated as shown in Fig. 15. Transmission characteristics of FSS devices can be measured through a few methods [25, 26]. The measurement setup for the proposed FSS is shown in Fig. 16. Two horn antennas and a vector network analyzer were used. The experiment setup is composed of two broadband SATIMO horn antennas which are pointing to each other. The FSS under test is placed between the antennas. The distance is large enough to be considered as in the far field region of the horn (meeting > $2D^2/\lambda$ condition), where D is the antenna size and λ is the free space wavelength at the resonant frequency. Thus the wave arriving at the FSS can be considered as a plane wave. To avoid spillover or diffraction at the edge of the FSS, RF absorbing materials are used around the edges. In order to ensure the measurement accuracy, a calibration was carried out. Without the FSS, the transmission coefficient was first measured as the reference for 100% transmission (S_{21} = 1 or 0 dB). When the FSS is under test, the measured transmission coefficient was normalized to the reference. In order to measure the transmission at different incident angles, the FSS holder fixture can be rotated to the angle of interest. In this case the measurement accuracy is not as good as the normal incident angle due to the limited size of the FSS.

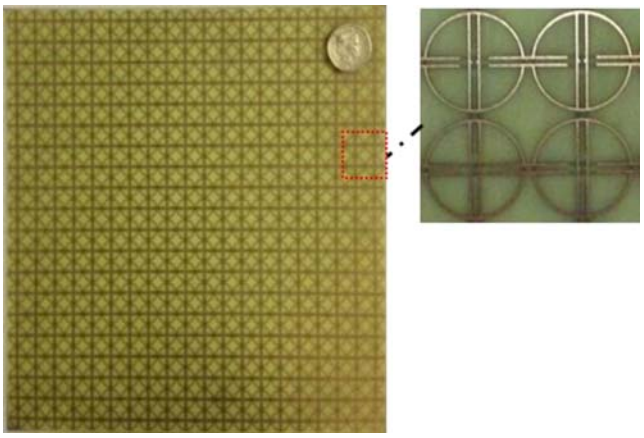

Fig. 15. A photograph of the fabricated FSS with the proposed miniaturized array elements.

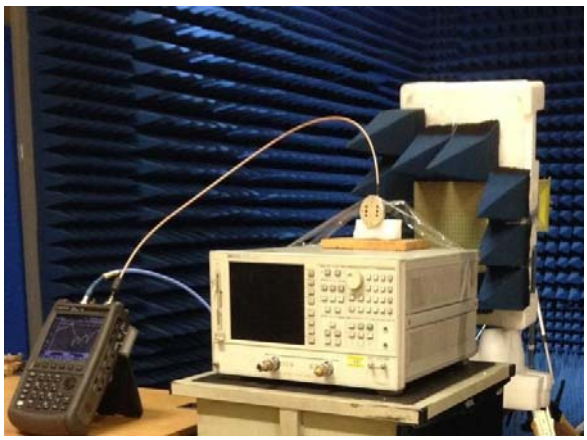

Fig. 16. The experimental setup to measure the transmission coefficient of the FSS.

The phase error can be calculated using the path length difference between the center and the edge. The formula to calculate the phase difference across the aperture is the distance difference•$2\pi/\lambda$ which is a function of the wavelength. Typically it should be smaller than 90 degrees.

Ideally the array size should be as large as possible. Since the measurement is a comparative one (compared with the response without the FSS), the array size of 200 mm × 200 mm (1.45λ × 1.45λ) consisting of 20 × 20 elements appeared to be large enough to give reliable results.

The line of sight between the two antennas passes through the centre of the FSS prototype. The antennas are aligned to ensure the formation of uniform plane wave impinging upon the FSS structure. Measurement of the fabricated FSS is performed in two steps. Firstly, the transmission response of the system without the FSS is measured. This measurement result is used to calibrate the FSS response. Secondly, the transmission coefficient S_{21} was measured at various angles of incidence and polarization. The measured results of the miniaturized FSS are shown in Fig. 17 and Fig. 18. They show a good agreement with the simulated ones. The frequency response of the proposed FSS is insensitive to the angle of incidence, as shown in Fig. 17. It demonstrates a measured

This article has been accepted for publication in a future issue of this journal, but has not been fully edited. Content may change prior to final publication. Citation information: DOI 10.1109/TAP.2017.2684199, IEEE Transactions on Antennas and Propagation

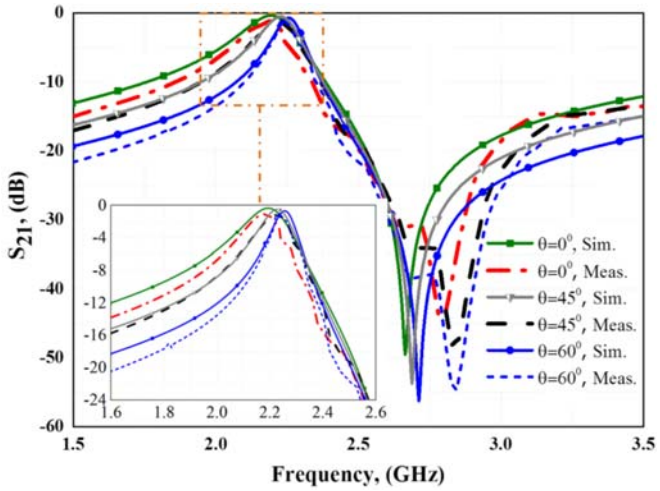

Fig. 17. The simulated and measured transmission coefficients of the miniaturized FSS structure at different incident angles.

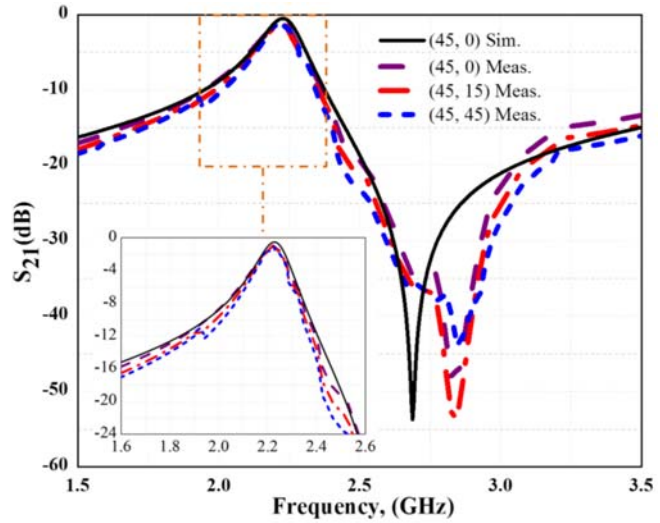

Fig. 18. The simulated and measured transmission coefficients of the miniaturized FSS structure under the 45° incident angle and various polarization angles.

insertion loss of about 0.72 dB at its resonant frequency for normal incidence, which is mainly attributed to the dielectric and the metallic losses of the structure. The measured result of the FSS with 45˚ incident angle and various polarization angles is shown in Fig. 18. It can be seen that good agreement between simulation and measurement has been achieved. The proposed miniaturized FSS exhibits almost the same response at different polarization angles with a fractional bandwidth of 9%. The measured insertion loss is about 0.92 dB for normal incidence, and 0.98 dB at 60˚ incident angle at its resonant frequency. This is comparable to the measured insertion losses in the references. For example, the measured insertion loss is about 0.7 dB at the normal incident angle in [15], 0.47 dB in [16], and 1.2 dB in [18].

IV. Conclusion

A few novel approaches have been combined in this paper to miniaturize FSS elements and make the FSS insensitive to the angle of incident waves. The interconnection of the array elements in one direction can change the equivalent circuit of the FSS structure, and increase the values of the equivalent circuit component values.

In the proposed design, two layers on two sides of a substrate are arranged orthogonal to each other in the xy-plane to build up the FSS. As a result, a very strong cross-layer capacitance will be generated between the two layers. The cross-layer capacitance can miniaturize the element much further. It can offer further significant advantages because the FSS with a low-profile substrate would have a lower resonant frequency. An analytical circuit model has been presented to describe the miniaturized FSS. The proposed design has the smallest size compared to other miniaturized designs.

Furthermore, using the proposed method, the array element in the FSS does not have to be rotationally symmetrical by 90°. The method can be easily adopted in a multi-layer FSS design. The proposed structure has been fabricated and tested. It has been shown that, by interconnecting adjacent resonators in one direction and having two orthogonal layers, the resonant frequency of the array was reduced from 5.5 GHz to 2.32 GHz. When the substrate thickness is reduced from 0.8 mm to 0.127 mm, the resonant frequency is lowered further from 2.32 GHz to 1.35 GHz. One FSS was fabricated on a 0.6 mm thick FR4 to validate the theory. The FSS was tested under different incident wave angles. It was verified that the response is insensitive to the incident angle. It exhibits polarization insensitivity for different incident angles. In future work, a wideband performance can be achieved by revising the element structure if desired. The proposed method can also be used for multi-layer FSS design.

References

[1] R. Ott, R. Kouyoumjian, and L. Peters, “Scattering by a Two-Dimensional Periodic Array of Narrow Plate,” *Radio Science,* vol. 2, no. 11, pp. 1347-1359, 1967.

[2] B. Munk, and R. Luebbers, “Reflection properties of two-layer dipole arrays,” *IEEE Trans. Antennas Propag.,* vol. 22, no. 6, pp. 766-773, 1974.

[3] J. C. Vardaxoglou, *Frequency selective surfaces: analysis and design*: Research Studies Press, 1997.

[4] B. A. Munk, "Frequency selective surfaces theory and design. john Wiley&Sons," Inc, 2000.

[5] S.-W. Lee, “Scattering by dielectric-loaded screen,” *IEEE Trans. Antennas Propag.,* vol. 19, no. 5, pp. 656-665, 1971.

[6] F. Sakran, Y. Neve-Oz, A. Ron, M. Golosovsky, D. Davidov, and A. Frenkel, “Absorbing frequency-selective-surface for the mm-wave range,” *IEEE Trans. Antennas Propag.,* vol. 56, no. 8, pp. 2649-2655, Aug, 2008.

[7] S. Chakravarty, R. Mittra, and N. R. Williams, “On the application of the microgenetic algorithm to the design of broad-band microwave absorbers comprising frequency-selective surfaces embedded in multilayered dielectric media,” *IEEE Trans. Microw. Theory Techn.,* vol. 49, no. 6, pp. 1050-1059, Jun, 2001.

[8] V. D. Agrawal, and W. A. Imbriale, “Design of a Dichroic Cassegrain Subreflector,” *IEEE Trans. Antennas Propag.,* vol. 27, no. 4, pp. 466-473, 1979.

[9] Y. Rahmatsamii, and A. N. Tulintseff, “Diffraction Analysis of Frequency-Selective Reflector Antennas,” *IEEE Trans. Antennas Propag.,* vol. 41, no. 4, pp. 476-487, Apr, 1993.

[10] T. K. Wu, “Cassini Frequency-Selective Surface Development,” *Journal of Electromagnetic Waves and Applications,* vol. 8, no. 12, pp. 1547-1561, 1994.

[11] D. Sievenpiper, L. J. Zhang, R. F. J. Broas, N. G. Alexopolous, and E. Yablonovitch, “Comments on "High-impedance electromagnetic surfaces with a forbidden frequency band" - Authors' reply,” *IEEE*

Trans. Microw. Theory Techn., vol. 49, no. 1, pp. 228-228, Jan, 2001.

[12] F. Costa, A. Monorchio, and G. Manara, "Efficient Analysis of Frequency-Selective Surfaces by a Simple Equivalent-Circuit Model," *IEEE Antennas and Propagation Magazine,* vol. 54, no. 4, pp. 35-48, Aug, 2012.

[13] R. Ulrich, "Far-Infrared Properties of Metallic Mesh and Its Complementary Structure," *Infrared Physics,* vol. 7, no. 1, pp. 37-&, 1967.

[14] K. Sarabandi, and N. Behdad, "A frequency selective surface with miniaturized elements," *IEEE Trans. Antennas Propag.,* vol. 55, no. 5, pp. 1239-1245, May, 2007.

[15] C. N. Chiu, and K. P. Chang, "A Novel Miniaturized-Element Frequency Selective Surface Having a Stable Resonance," *IEEE Antennas Wireless Propag. Lett.,* vol. 8, pp. 1175-1177, 2009.

[16] F. C. Huang, C. N. Chiu, T. L. Wu, and Y. P. Chiou, "A Circular-Ring Miniaturized-Element Metasurface With Many Good Features for Frequency Selective Shielding Applications," *IEEE Transactions on Electromagnetic Compatibility,* vol. 57, no. 3, pp. 365-374, Jun, 2015.

[17] S. N. Azemi, K. Ghorbani, and W. S. T. Rowe, "Angularly Stable Frequency Selective Surface With Miniaturized Unit Cell," *IEEE Microwave and Wireless Components Letters,* vol. 25, no. 7, pp. 454-456, Jul, 2015.

[18] G. H. Yang, T. Zhang, W. L. Li, and Q. Wu, "A Novel Stable Miniaturized Frequency Selective Surface," *IEEE Antennas Wireless Propag. Lett.,* vol. 9, pp. 1018-1021, 2010.

[19] M. B. Yan, S. B. Qu, J. F. Wang, J. Q. Zhang, A. X. Zhang, S. Xia, and W. J. Wang, "A Novel Miniaturized Frequency Selective Surface With Stable Resonance," *IEEE Antennas Wireless Propag. Lett.,* vol. 13, pp. 639-641, 2014.

[20] N. Marcuvitz, *Waveguide handbook*: Iet, 1951.[21] G. Parker, "What is the capacitance of parallel plates?," *Computers in Physics,* vol. 5, no. 5, pp. 534-540, 1991.

[22] G. Carlson, and B. Illman, "The circular disk parallel plate capacitor," *American Journal of Physics,* vol. 62, no. 12, pp. 1099-1105, 1994.

[23] L. D. Landau, and E. Lifshitz, *Course of Theoretical Physics. Vol. 8: Electrodynamics of Continuous Media*: Oxford, 1960.

[24] R. J. Langley, and E. A. Parker, "Equivalent-Circuit Model for Arrays of Square Loops," *Electronics Letters,* vol. 18, no. 7, pp. 294-296, 1982.

[25] T. Cwik, R. Mittra, K. Lang, and T. Wu, "Frequency selective screens," *IEEE Antennas and Propagation Society Newsletter,* vol. 29, no. 2, pp. 5-10, 1987.

[26] D. K. Ghodgaonkar, V. V. Varadan, and V. K. Varadan, "A free-space method for measurement of dielectric constants and loss tangents at microwave frequencies," *IEEE Transactions on Instrumentation and measurement,* vol. 38, no. 3, pp. 789-793, 1989.

MUAAD NASER HUSSEIN was born in Basra, Iraq. He received the B.Sc. and M.Sc. degrees in electrical engineering from the University of Basra, Iraq, in 2002 and 2005, respectively. He is currently pursuing the Ph.D. degree in electrical engineering and electronics with the University of Liverpool, U.K. He was a Microwave Engineer with ASIACELL Telecom., Sulaimaniyah, Iraq, for seven years. He has been a Lecturer with the Department of Electrical Power Engineering, South Technical University, Basra, Iraq. His research interests focus on frequency selective surfaces, wireless power transfer, and antenna design.

Jiafeng Zhou received a B.Sc. degree in Radio Physics from Nanjing University, Nanjing, China, in 1997, and a Ph.D. degree from the University of Birmingham, Birmingham, U.K., in 2004. His doctoral research concerned high-temperature superconductor microwave filters.

From July 1997, for two and a half years he was with the National Meteorological Satellite Centre of China, Beijing, China, where he was involved with the development of communication systems for Chinese geostationary meteorological satellites. From August 2004 to April 2006, he was a Research Fellow with the University of Birmingham, where his research concerned phased arrays for reflector observing systems. Then he moved to the Department of Electronic and Electrical Engineering, University of Bristol, Bristol, U.K until August 2013. His research in Bristol was on the development of highly efficient and linear amplifiers. He is now with the Department of Electrical Engineering and Electronics, University of Liverpool, Liverpool, UK. His current research interests include microwave power amplifiers, filters, electromagnetic energy harvesting and wireless power transfer.

Yi Huang (S'91 – M'96 – SM'06) received BSc in Physics (Wuhan University, China) in 1984, MSc (Eng) in Microwave Engineering (NRIET, Nanjing, China) in 1987, and DPhil in Communications from the University of Oxford, UK in 1994.

He has been conducting research in the areas of wireless communications, applied electromagnetics, radar and antennas since 1987. His experience includes 3 years spent with NRIET (China) as a *Radar Engineer* and various periods with the Universities of Birmingham, Oxford, and Essex at the UK as a member of research staff. He worked as a *Research Fellow* at British Telecom Labs in 1994, and then joined the Department of Electrical Engineering & Electronics, the University of Liverpool, UK as a *Faculty* in 1995, where he is now a full *Professor in Wireless Engineering*, the *Head of High Frequency Engineering Group and Deputy Head of Department*.

Prof Huang has published over 300 refereed papers in leading international journals and conference proceedings, and authored *Antennas: from Theory to Practice* (John Wiley, 2008) and *Reverberation Chambers: Theory and Applications to EMC and Antenna Measurements* (John Wiley, 2016). He has received many research grants from research councils, government agencies, charity, EU and industry, acted as a consultant to various companies, and served on a number of national and international technical committees and been an *Editor, Associate Editor or Guest Editor* of four of international journals. He has been a *keynote/invited speaker* and *organiser* of many conferences and workshops (e.g. WiCom 2006, 2010, IEEE iWAT2010, and LAPC2012). He is at present the *Editor-in-Chief* of Wireless Engineering and Technology, *Associate Editor* of IEEE Antennas and Wireless Propagation Letters, *UK and Ireland Rep* to European Association of Antenna and

Propagation (EurAAP), a *Senior Member* of IEEE, *Senior Fellow* of HEA, and a *Fellow* of IET.

Muayad Kod received the B.Sc. and M.Sc. degrees from the Department of Electronics and Communications, Al-Nahrain University, Baghdad, Iraq, in 2002 and 2005, respectively. He received the Ph.D. degree from the Department of Electrical Engineering and Electronics, The University of Liverpool, Liverpool, U.K, in 2016.

He was an OMC Engineer with Global Telecom Holding/Iraqna, Baghdad, Iraq, in 2005. In 2007, he joined Asiacell, Sulaimaniyah, Iraq, as a Radio Frequency (RF) Engineer, where he was involved in telecommunication, and moved to Omnnea, Najaf, Iraq, as an RF Engineering Team Leader in 2008, where he was involved in wireless telecommunications. Since 2009, he has been a Lecturer with the Department of Electrical Engineering and Electronics, University of Kerbala, Karbala, Iraq. His current research interests include wireless power transfer and telemetry to implantable medical devices, wearable and implantable antennas, RFID, energy harvesting and frequency selective surfaces.

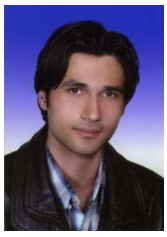

Abed Pour Sohrab was born in Bandar Anzali, Iran. He received the BSc degree in electrical engineering from K. N. Toosi University of Technology, Tehran, Iran, in 2008 and the MSc degree in electromagnetics and antenna engineering from Tarbiat Modares University, Tehran, Iran, in 2012. He is currently pursuing the PhD degree in electrical engineering at University of Liverpool, UK. His research interests include frequency selective surfaces, electromagnetic absorbers, UHF RFID tags and novel antenna designing.